Received: 21 May 2018 | Revised: 17 October 2018 | Accepted: 18 October 2018

DOI: 10.1111/gbi.12323

ORIGINAL ARTICLE

WILEY gebiology

A small marine biosphere in the Proterozoic

Thomas A. Laakso | Daniel P. Schrag

Department of Earth and Planetary Sciences, Harvard University, Cambridge, Massachusetts

Correspondence
Thomas A. Laakso, Department of Earth and Planetary Sciences, Harvard University, Cambridge, MA.
Email: laakso@fas.harvard.edu

Funding information
National Aeronautics and Space Administration, Grant/Award Number: NNX11AP89H

Abstract

The riverine supply of the globally limiting nutrient, phosphorus, to the ocean accounts for only a few percent of nutrient supply to photosynthetic organisms in surface waters. Recycling of marine organic matter by heterotrophic organisms provides almost all of the phosphorus that drives net primary production in the modern ocean. In the low-oxygen environments of the Proterozoic, the lack of free oxygen would have limited rates of oxic respiration, slowing the recycling of nutrients and thus limiting global rates of photosynthesis. A series of steady-state mass balance calculations suggest that the rate of net primary production in the ocean was no more than 10% of its modern value during the Proterozoic eon, and possibly less than 1%. The supply of nutrients in such a world would be dominated by river input, rather than recycling within the water column, leading to a small marine biosphere found primarily within estuarine environments.

1 | INTRODUCTION

Photosynthetic organisms in the modern ocean fix approximately 4,000 Tmol of CO_2 to organic carbon every year (Field, Behrenfeld, Randerson, & Falkowski, 1998), accounting for nearly half of global net primary production (NPP). More than 99% of the resulting organic carbon is reoxidized in the water column or in sediments (Hedges & Keil, 1995), supporting heterotrophic communities in a wide variety of environments, and exerting a major influence on the distribution of oxygen in the water column. Organic carbon availability also governs the cycling of sulfur and iron in sedimentary systems, which influence global redox budgets and generate many of the chemical and isotopic records that record information about both ancient and modern ocean chemistry (e.g. Fike, Bradley, & Rose, 2015; Poulton & Canfield, 2011). Understanding how the rate and spatial distribution of carbon fixation may have changed over Earth history can shed critical light on the biogeochemical structure of the ancient ocean. This is of particular interest for studying the Proterozoic, when redox proxies suggest that the concentration of oxygen in the atmosphere was no more than ~10% modern levels, and possibly much less during the Mesoproterozoic (Planavsky et al., 2014). Sedimentary records suggest a complex redox structure in the ocean, with oxic surface waters giving way to zones of euxinia and ferruginous deep waters (Poulton, Fralick, & Canfield, 2010; Sperling et al., 2015). The distribution of nutrients and organic material in the Proterozoic ocean likely played a role in creating these patterns, and in determining the structure of marine ecosystems (e.g., Johnston et al., 2012).

The rate of net primary production is determined by the supply of nutrients, in particular phosphorus, to the photic zone. Though nitrogen and iron may be locally or transiently limiting, phosphorus is thought to be the globally limiting nutrient today, as diazotrophic primary producers can access the vast pool of atmospheric N_2 in the event of nitrogen scarcity (Tyrrell, 1999), an argument that likely holds for Proterozoic environments as well (Laakso & Schrag, 2018). Bioavailable phosphate ions are supplied to the oceans via weathering of apatite, but at a rate of <300 Gmol P/year (Benitez-Nelson, 2000), enough to support less than 1% of modern productivity. The remaining 99% of carbon fixation is instead associated with recycled phosphorus: organic phosphorus is remineralized during heterotrophy in the water column and sediments, and then returned to the photic zone via upwelling where it can be reused. Zones of intense upwelling are therefore associated with intense productivity, but diffuse upwelling of a well-mixed, deep ocean P reservoir allows for productivity to occur in pelagic waters, which in fact dominate total productivity (Dunne, Sarmiento, & Gnanadesikan, 2007). Efficient recycling of nutrients is therefore central in setting the rate and structure of NPP in the modern ocean.

The rate of phosphorus recycling has likely varied over Earth history, because remineralization rates generally depend on the availability of

oxygen. In low-O_2 environments, slower remineralization kinetics allow a larger proportion of organic material to sink through the water column (Van Mooy, Keil, & Devol, 2002) and be buried in sediments (Katsev & Crowe, 2015). This suggests that, in periods of Earth history when oxygen levels were low, a smaller fraction of organic matter would have been remineralized, leading to lower rates of phosphorus recycling and net primary production, and a reduced importance of upwelling in setting the spatial pattern of NPP. The Proterozoic and Archean eons had atmospheric oxygen levels of roughly 1% and <0.001% of present-day levels, respectively (see Lyons, Reinhard, & Planavsky, 2014; for a summary), suggesting potentially very large changes to remineralization, and thus to productivity (Kipp & Stüeken, 2017).

There are many challenges to arriving at a more quantitative assessment of the relationship between O_2 and NPP. Any changes in organic carbon cycling have implications for the oxygen and phosphorus budgets, both of which must remain balanced on long timescales. Kipp and Stüeken (2017) recently argued that efficient burial of organic material in the oxidant-poor Precambrian oceans would have reduced oceanic phosphorus concentrations, suppressing productivity and thus pO_2. However, the increase in organic burial would itself have led to additional oxygen production, so it is not clear that the proposed qualitative budget is balanced on geological timescales. In this study, we calculate rates of net primary production that are consistent with balanced global budgets for oxygen and phosphorus in the low-oxygen environments of the Proterozoic.

2 | MODEL AND METHODS

We explore this problem using two simple conceptual models of the phosphorus and oxygen cycles, developed below. We also compare these results to a recently published model of ocean/atmosphere biogeochemistry, which explicitly tracks the coupled cycles of O_2, P, Fe, S, H_2, and CH_4 (Laakso & Schrag, 2017).

2.1 | Global mass balance

The first conceptual model is a simple global mass balance for P and O_2 that yields a simple expression for NPP in terms of oxygen-sensitive carbon cycling processes. A mass balance approach ensures calculations of NPP are for steady-state conditions given a particular oxygen level. We use this model to place bounds on the magnitude of NPP at different points in Earth history.

A steady-state oxygen cycle balances the oxygen source, burial of organic carbon, against various oxidative sinks:

$$\varepsilon_{org}\mathrm{NPP} = g(pO_2) \tag{1}$$

where NPP is the rate of net primary production in mol C/year. ε_{org} is the fraction of net primary production that is ultimately buried in marine sediments, again measured in mol C/year, and the sink function, g, is a monotonically increasing function of atmospheric pO_2 representing the globally averaged oxidation kinetics of reduced iron, sulfur, carbon, and volcanic gases. Some processes, such as subaerial pyrite oxidation (Holland, 1984) and H_2 oxidation in the atmosphere (Goldblatt, Lenton, & Watson, 2006), are not monotonically increasing functions of oxygen concentration. However, these are either insensitive to or vary relatively weakly with pO_2 at levels above those of the Archean. This suggests that the sink for oxygen, g, was smaller during the moderately oxygenated Proterozoic than during the highly oxidized Phanerozoic. Therefore, low levels of oxygen could only have been sustained through the Proterozoic if the source of oxygen was also smaller than it is today:

$$\varepsilon'_{org}\mathrm{NPP}' < \varepsilon_{org}\mathrm{NPP} \tag{2}$$

where x denotes a value in the Phanerozoic, and x' its value during the Proterozoic. In order to understand how ε_{org} may have varied over time, we decompose it into two factors, $\varepsilon_{org} = f_1 f_2$. The term f_1 is the "export efficiency", or the fraction of net primary production, measured in terms of organic carbon, that is delivered to the sediments. f_2 is the "burial efficiency", or the fraction of the organic carbon delivered to sediments that is ultimately buried. The relative rate of net primary production is then given by:

$$\frac{\mathrm{NPP}'}{\mathrm{NPP}} < \frac{f_1 f_2}{(f_1 f_2)'} \tag{3}$$

Both the export and burial efficiencies increase in low-oxygen environments (see Section 4.1 for a detailed discussion), implying that rates of net primary production were likely lower during the Proterozoic than they were today. Rates of net primary production are controlled by the rate of supply of the limiting nutrient, assumed to be phosphorus during the Proterozoic (Laakso & Schrag, 2018). To ensure Equation (3) is consistent with a closed phosphorus budget, we next consider a steady-state P cycle.

Phosphorus is introduced to the marine system primarily by weathering of apatite. A portion of this P is in the form of detrital minerals or is adsorbed to particulates and is not bioavailable. We will ignore this portion of the supply, and focus on the bioavailable supply of weathered P, while noting that the bioavailability of weathered P has likely varied over geologic time. This input must be balanced by burial of P. Organic matter is the dominant shuttle for P out of the oceans (Benitez-Nelson, 2000), such that the gross flux of P out of the ocean is equal to the rate of organic carbon deposition multiplied by the average C:P ratio of organic matter produced in the ocean. However, net P burial can become decoupled from organic carbon burial both by preferential remineralization of P-rich organic compounds and by precipitation of authigenic phosphorus mineral phases following remineralization (Ruttenberg & Berner, 1993). Therefore, steady-state phosphorus cycling can be written as:

$$W_P = \frac{\varepsilon_{org}\mathrm{NPP}}{\rho} \tag{4}$$

where W_P is the rate of bioavailable phosphorus release via weathering measured in mol P/year, and ρ is a globally averaged ratio of organic carbon to total phosphorus in marine sediments. In general, anoxic sediments retain less P due to some combination of preferential remineralization of P-rich compounds (Van Cappellen & Ingall,

1996) and to less efficient retention of remineralized P (Colman & Holland, 2000). Though the relative roles of the two effects remain debated (e.g., Anderson, Delaney, & Faul, 2001), sedimentary C_{org}:P_{Σ} ratios, where P_{Σ} represents the sum of both organic and inorganic phosphorus phases in the sediment, are oxygen-sensitive (Algeo & Ingall, 2007). Note that these global budgets do not depend on the C:P ratio of organic matter directly, but rather on the ratio of organic carbon burial to total P burial, ρ.

Combining the steady-state oxygen (3) and phosphorus (4) budgets produce a set of internally consistent rules regarding biogeochemical cycling in the Proterozoic:

$$\frac{\mathrm{NPP}'}{\mathrm{NPP}} < \frac{f_1 f_2}{(f_1 f_2)'} \tag{5a}$$

$$\frac{W'_{\mathrm{P}}}{W_{\mathrm{P}}} < \frac{\rho}{\rho'} \tag{5b}$$

$$\frac{A'}{A} = \frac{f_1 f_2 \rho'}{(f_1 f_2)' \rho} \tag{5c}$$

where $A = \mathrm{NPP}/W_{\mathrm{P}}$, the rate of net primary productivity normalized to nutrient inputs from weathering. The first relationship describes the relative rates of net primary production that is consistent with a balanced oxygen budget, given changes in organic carbon cycling. The second relationship describes the change in the rate of phosphorus supply required to maintain that rate of NPP, while also allowing for redox-sensitive changes in sedimentary P cycling. The final relationship describes the weathering-normalized net primary production that is consistent with both budgets. It measures the amplification, A, of net primary production by nutrient recycling, relative to what is expected from weathering alone. For example, the amplification today is more than 10,000, indicating a world in which NPP is dominated by nutrients supplied via upwelling and remineralization in the photic zone, rather than by the riverine flux.

2.2 | Two-column mass balance

Changes in the relative importance of the riverine flux suggest a redistribution of NPP toward either river-influenced coastal waters or more distal pelagic waters. These two regions are associated with large differences in average sedimentation rate, which exerts an important control on organic carbon burial independent of redox effects (e.g., Katsev & Crowe, 2015). This suggests potential feedbacks: changes in the rate of net primary production could drive spatial redistributions of productivity that would then cause further changes in the rate of global NPP. To explore how these effects might influence our mass balance results, the model discussed above is generalized to a two-column representation of the ocean. This model is depicted schematically in Figure 1.

Column A represents coastal regions, with shallow water depth and relatively rapid rates of sedimentation (Sadler, 1999). Net primary production in this region is driven by a combination of coastal upwelling and direct input of nutrients from weathering.

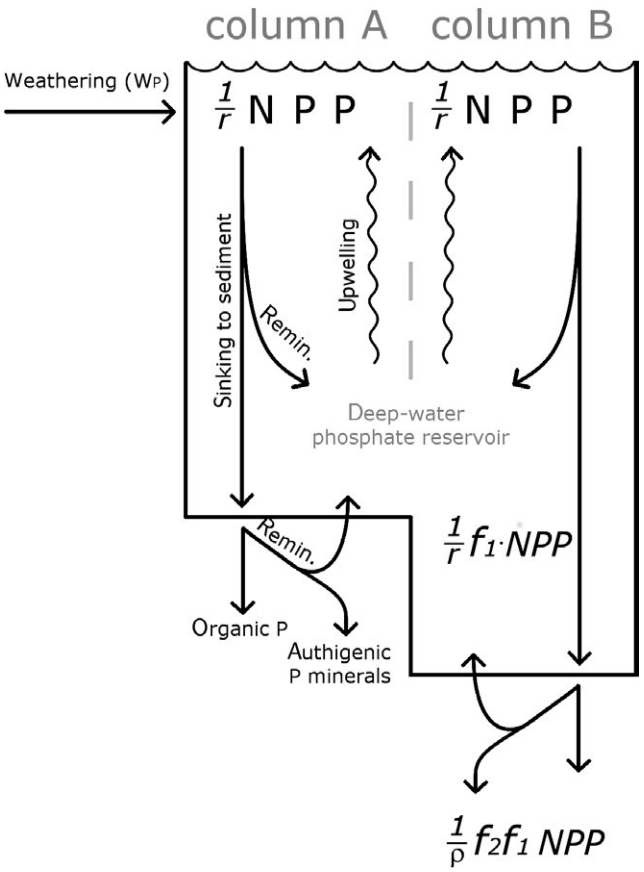

FIGURE 1 The two-column mass balance model. Each column is associated with its own values of NPP, f_1, f_2, and ρ, though these are not explicitly shown for clarity

Column B represents pelagic regions, characterized by deep water, relatively slow rates of sedimentation, and net primary production that is only driven by upwelling. Both columns are assumed to be in communication with a well-mixed deep-water reservoir of phosphate, which is fed by remineralization in both water columns, and by the diffusion of remineralized P from sediment porewaters. This implies that the steady-state rate of global phosphorus upwelling must be equal to the sum of all remineralization processes minus the rate of authigenic P mineral formation. A fraction μ of the upwelling volume circulates into the photic zone of column A, with the remainder upwelling in column B.

Note that this model does not account for recycling of nutrients directly in the photic zone, but forces all remineralized P to be redistributed via upwelling. This will tend to give a lower bound on the redistribution of productivity toward coastal areas. Assuming steady-state conditions, it is possible to solve for the amplification factor $\mathrm{NPP}/W_{\mathrm{P}}$ in terms of the column-specific cycling terms, f_1, f_2, and ρ, as shown in the Appendix A.

3 | RESULTS

We first calculate NPP using the global mass balance model. Figures 2–4 show steady-state NPP, W_{P}, and the amplification

NPP/W_P as a function of the export and burial efficiencies, and the $C_{org}:P_{\Sigma}$ ratio. For reference, the modern export and burial efficiencies are estimated at 1% and 10% respectively (Hedges & Keil, 1995). The $C_{org}:P_{\Sigma}$ ratio, ρ, is more difficult to constrain globally. Estimates based on sediment composition suggest approximately 90% of all P burial is in authigenic forms, suggesting a ρ value of ~10. Similarly, closing P mass balance (4) with modern rates of net primary productivity (4,000 Tmol C/year; Field et al., 1998) and riverine P inputs (~300 Gmol P/year; Benitez-Nelson, 2000) yields $\rho = 13$.

Figure 2 shows the maximum rate of net primary productivity consistent with a low-oxygen atmosphere. This rate decreases as either the export efficiency f_1 or the burial efficiency f_2 increases relative to its modern value (Figure 2). For Proterozoic values of these parameters (see Section 4), NPP is between 0.3% and 3% of its modern rate.

Figure 3 shows the maximum rate of bioavailable P supply to the ocean that is consistent with low-oxygen conditions. The weathering or bioavailability of P must decrease as the $C_{org}:P_{\Sigma}$ ratio in sediments, ρ, increases. Imposing values of ρ appropriate for low-oxygen conditions (see Section 4), the maximum permissible rate of P supply is between 4% and 13% of its modern value. A variety of mechanisms may drive this change, as discussed below.

Figure 4 shows the rate of NPP that can be sustained at a given rate of nutrient supply, the "amplification factor" $A = NPP/W_P$. At higher export and burial efficiencies, NPP/W_P decreases; at higher values of the $C_{org}:P_{\Sigma}$ ratio, NPP/W_P increases. The effects of f_1 and f_2 dominate over the effect of ρ, in the sense that the majority of the parameter space explored has amplification factors several times smaller than the modern value of ~10,000, ranging from 300 to 7,500.

We also calculate NPP in the two-column model, allowing burial and export efficiencies to vary away from modern values only in the pelagic realm; coastal burial efficiencies are fixed at $f_1 = 0.25$ and $f_2 = 0.3$ (based on Dunne et al., 2007). This reflects the relative insensitivity of shallow, rapidly accumulating sediments to variations in redox conditions (Katsev & Crowe, 2015). ρ is set to 13 in both columns. Figure 5 shows the change in weathering-normalized NPP for different values of the deep-water export efficiency. As burial of organic carbon becomes more efficient, P regeneration decreases and

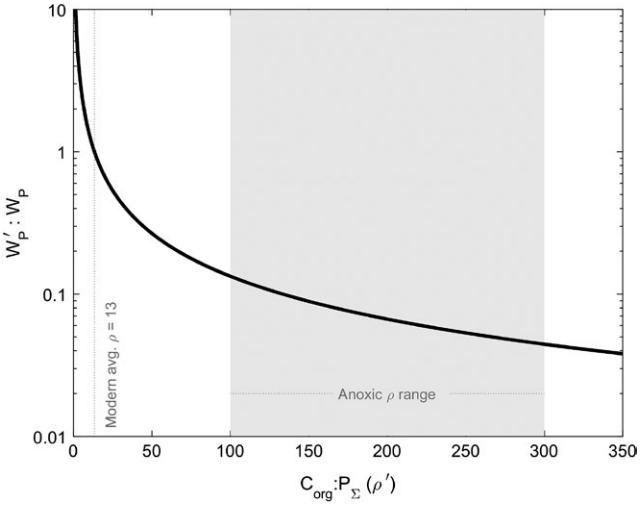

FIGURE 3 The maximum P weathering rate (W_P') consistent with a low-oxygen atmosphere, normalized to the modern rate (W_P). Modern conditions are represented by the dotted line. Proterozoic conditions are represented by ρ' values greater than 100

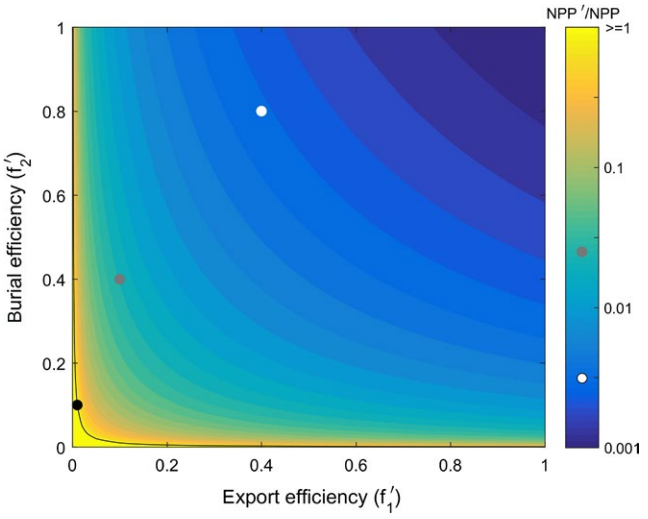

FIGURE 2 Contours of the maximum net primary production (NPP′) consistent with a low-oxygen atmosphere, normalized to the modern rate (NPP). Modern conditions are represented by the black point, with the black contour indicating conditions that give modern rates of NPP. Upper-bound (gray) and best-guess (white) estimates for Proterozoic NPP are shown by the other points [Colour figure can be viewed at wileyonlinelibrary.com]

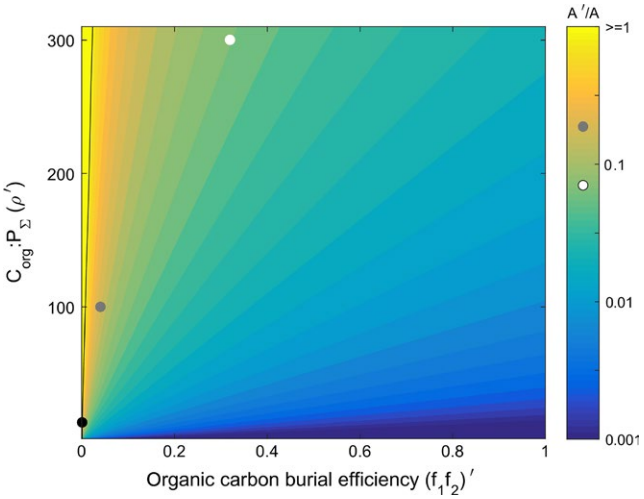

FIGURE 4 Contours of the amplification factor ($A' = NPP'/W_P'$), normalized to the modern factor (A), for different $C_{org}:P_{\Sigma}$ ratios (ρ) and total burial efficiencies (f_1f_2). Modern conditions are represented by the black point, with the black contour indicating conditions that give modern amplification factors. Upper-bound (gray) and best-guess (white) estimates for Proterozoic amplification are shown by the other points [Colour figure can be viewed at wileyonlinelibrary.com]

NPP shifts toward the shallow-water column, making it less sensitive to the oxygen-driven changes in pelagic carbon cycling. Therefore, NPP varies less strongly than in the global model.

4 | DISCUSSION

The magnitude of NPP must decrease as organic carbon is buried more efficiently (larger f_1 or f_2). This is a consequence of balancing the oxygen budget under low-oxygen conditions, when the rate of oxygen loss is generally lower. To prevent unbalanced oxygen generation, the rate of organic carbon burial must also be lower. This is only possible if the large burial efficiencies found in anoxic environments are offset by low rates of NPP. The rate of organic carbon burial also sets the rate of P burial for a given value of the C_{org}:P_{Σ} ratio (ρ) in sediments. At steady state, bioavailable P input via weathering must be equal to burial, so the larger values of ρ expected in an anoxic world require lower rates of phosphorus weathering in order to maintain steady state. Changes in both NPP and weathering will influence the fraction of productivity that is fueled by riverine input, rather than nutrient regeneration, potentially altering the spatial distribution of net primary production.

All these cycling processes—export, burial, and regeneration for both C and P—are oxygen sensitive, suggesting that productivity and nutrient supply may have varied, potentially by orders of magnitude (Figures 2–4), as oxygen levels varied over Earth history. However, the sign and magnitude of these changes differ between processes.

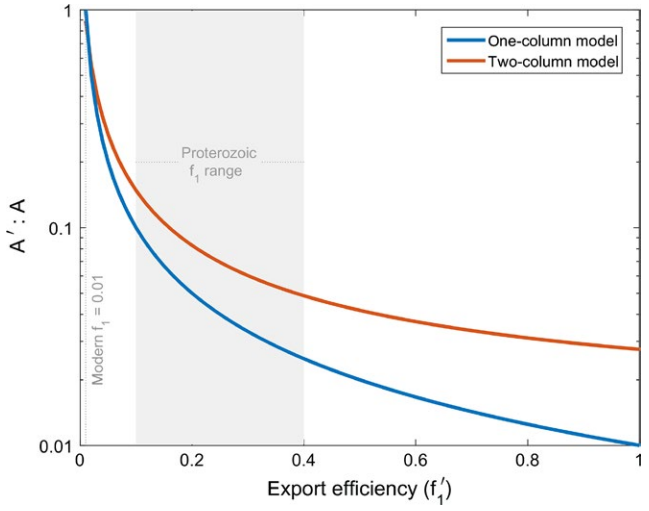

FIGURE 5 Net primary production, normalized to weathering, calculated in both the global and two-column models, for variations in f_1, the export efficiency. "f_1" here refers to its global value in the global model and its pelagic value in the two-column model. The "modern" value of f_1 is chosen to give a global average burial of 0.01 in both cases. All calculations have a globally averaged f_2 of 0.1, and ρ = 13. Coastal production is dominated by riverine inputs of nutrients, μ = 0 [Colour figure can be viewed at wileyonlinelibrary.com]

4.1 | Carbon cycling in a low-oxygen world

Organic carbon is buried more efficiently in low-oxygen environments (e.g., Hartnett et al., 1998; Katsev & Crowe, 2015) such as those of the Proterozoic and Archean. Some authors have argued that burial efficiency is not particularly sensitive to oxygen concentrations, due increased activity by methanogens in low-oxygen and particularly low-sulfate environments (e.g., Habicht, Gade, Thamdrup, Berg, & Canfield, 2002; Pavlov, Hurtgen, Kasting, & Arthur, 2003). However, results from modern marine sediments (Katsev & Crowe, 2015) and from anoxic, sulfate-poor lakes such as Lake Matano (Kuntz, Laakso, Schrag, & Crowe, 2015), are consistent with increased burial efficiency in environments poor in electron acceptors. Lake Matano, for example, has burial efficiencies of more than 80%, relative to the material exported from the oxidized surface layer (Kuntz et al., 2015). This very high burial efficiency is maintained despite ongoing methanogenesis, which is in fact the dominant pathway of organic carbon degradation (Kuntz et al., 2015). These observations suggest that burial efficiencies in the low-sulfate, ferruginous oceans of the Proterozoic (Kah, Lyons, & Frank, 2004; Poulton & Canfield, 2011) may have been quite high. In the Archean eon, when surface oxygen concentrations were many orders of magnitude smaller than they are today (Pavlov & Kasting, 2002), and at least 100 times lower than during the Proterozoic (Planavsky et al., 2014), burial efficiencies may have been higher still.

While environments like Lake Matano provide one estimate of burial efficiencies in the Proterozoic, we can use modern oxygen-poor (but sulfate-rich) marine settings to find *lower* bounds on ancient burial efficiencies, and thus upper bounds on NPP. The export of biomass through the water column to the seafloor becomes more efficient in low-oxygen environments (i.e., f_1 increases). The degree of organic matter preservation as it sinks through the water column is typically expressed in terms of a power law, following Martin, Knauer, Karl, and Broenkow (1987), which relates the flux of sinking organic matter, *F*, to depth:

$$F(z) = F_0 z^{-b}$$

where F_0 is the organic flux at 100 m depth, and *z* is the depth expressed in hundreds of meters. Van Mooy et al. (2002) find that the attenuation coefficient *b* in a suboxic water column is only half the value of the global average taken over oxic waters (0.4 vs. 0.8). These values can be used to compare oxic and suboxic water columns, but Martin's law is not meant to apply in the photic zone, where competing production and respiration make export rates more difficult to determine. However, if one assumes the average depth of net primary production is 10 m, the power law yields an export efficiency of 20% at 100 m, and 1% export to the average seafloor depth of 4,000 m, both consistent with observations (e.g., Dunne et al., 2007). Applying the low-oxygen attenuation coefficient gives 40% export from the surface and 10% burial at the seafloor; despite the relatively large rate of oxidation in the surface ocean, overall burial efficiency f_1 increases tenfold.

This is likely a lower bound on export in the Proterozoic. Though debate continues over the exact level of pO_2 in the Proterozoic

atmosphere (e.g., Planavsky et al., 2014), and over the prevalence of deep-water euxinia (e.g., Sperling et al., 2015), the entire Proterozoic water column was likely less oxidized than the modern suboxic water mass used to derive our "low-oxygen" organic turnover rates. Van Mooy et al. (2002) calculate their attenuation coefficients from a site off the Pacific coast of Mexico, where oxygen levels do approach zero for several hundred meters, but increase again to almost 50 μM at depth. This oxygen level exceeds even the upper bound on Proterozoic surface waters (Sperling et al., 2015). It also reflects conditions that are almost certainly more oxidizing than the Precambrian deep ocean. Both ophiolites (Stolper & Keller, 2018) and iron speciation (Poulton & Canfield, 2011) indicate that the Proterozoic deep ocean was anoxic and ferruginous, and sulfate levels were most likely less than today (Kah et al., 2004). The lack of oxidants suggests more efficient organic carbon burial (Katsev & Crowe, 2015; see also Kipp & Stüeken, 2017) even if methanogenesis rates were elevated in the oxidant-poor environment (e.g., Kuntz et al., 2015). Both our deep-water export and global burial efficiencies are therefore likely to be underestimated.

The preservation of organic matter in the sediments is also typically more efficient in low-oxygen environments due to slower remineralization kinetics or decreased oxygen exposure time (i.e., f_2 increases; e.g., Hartnett, Keil, Hedges, & Devol, 1998). A comparison of modern oxic and euxinic sediments suggests that sediments underlying oxygen-free waters can have burial efficiencies more than ten times greater than oxic sediments, though the effect becomes weaker for larger sedimentation rates (Canfield, 1994). Using fits to this data (Katsev & Crowe, 2015), a modern global value of the burial efficiency (10%) is best represented by oxic sediments with a sedimentation rate of roughly 0.01 g cm^{-2} $year^{-1}$. Anoxic sediments with a similar sedimentation rate have a burial efficiency of ~40% or a fourfold increase.

These modern euxinic sediments are not likely to be representative of Proterozoic conditions, as they generally have high-sulfate water diffusing downward, which supplies an alternate electron acceptor for degrading organic carbon. For comparison, Lake Matano, which has a sedimentation rate of order 0.01 g cm^{-2} $year^{-1}$, has burial efficiencies in the range 80%–90% (Kuntz et al., 2015), so the results from modern marine environments are likely to be a lower bound on burial rates.

The C_{org}:P_{Σ} ratio, ρ, in sediment, is the result of several different physical processes. Following deposition of organic matter, remineralization liberates both C and P to porewater, but not necessarily in the same ratio at which they are deposited; early preferential remineralization of P-rich compounds, for example, appear to cause a spike in the C:P ratio of the remaining organic matter in immature sediments, though this typically relaxes back toward lower values over time (Anderson et al., 2001). Inorganic P may then either diffuse back to the water column or be retained in authigenic minerals such as fluorapatite (e.g., Ruttenberg & Berner, 1993). The net result of these processes appears to depend on a number of factors including redox state, sedimentation rate, and degree of bioturbation. Nevertheless, most observations suggest that the retention of P increases under more oxic conditions (Algeo & Ingall, 2007), at least in part due to more efficient trapping of phosphate via sorption to iron particles (Colman & Holland, 2000). Though individual sites may show both very high and very low ratios (e.g., Anderson et al., 2001), a compilation of sediments by Algeo and Ingall (2007) show an average increase in C_{org}:P_{Σ} from ~10 in highly oxidized sediments, suggesting extensive remineralization and trapping of P, to 100–300 in euxinic basins, suggesting remineralization of P-rich compounds followed by some degree of diffusive loss to the water column. Though ρ is not directly coupled to the C:P ratio of freshly deposited organic matter, a biologically mediated increase in this ratio in response to nutrient-poor conditions (e.g., Reinhard et al., 2017, and discussion below), may have translated into additional overall increases in C_{org}:P_{Σ}.

4.2 | The rate of productivity in a low-oxygen world

Given that export and burial efficiencies do increase under low-oxygen conditions, how small was NPP in the Proterozoic? Using the lower bounds on burial efficiency for a low-oxygen, ferruginous ocean (export efficiency $f_1 > 0.1$, burial efficiency $f_2 > 0.4$), the rate of net primary production in the Proterozoic must have been more than 40 times slower than it is today. Lake Matano provides a more realistic estimate. If the remineralization observed below the photic zone occurs entirely in the sediment, the sedimentary recycling efficiency is only 20%, while the extrapolated Martin curve discussed suggests photic zone recycling efficiency of 60% ($f_1 = 0.4$, $f_2 = 0.8$). This yields a weathering-normalized NPP rate that is more than 300 times slower than today.

These small rates of net primary production are required to balance the O_2 budget under Proterozoic oxygen levels, but such steady-state constraints do not describe the mechanism by which NPP was maintained at such low levels. Kipp and Stüeken (2017) recently pointed out that a shortage of electron acceptors before the Phanerozoic would necessarily lead to nutrient-depleted deep waters, low rates of P upwelling, and thus reduced NPP. This is consistent with our calculations, based on closing the redox budget under variable remineralization rates. However, these changes to the carbon cycle imply changes to phosphorus cycling that are not necessarily at steady state, and so cannot be considered in isolation. The decrease in P retention expected in the low-oxygen environment suggests that, if organic carbon burial is reduced (or even kept constant) by trade-offs between NPP and burial efficiency, P will accumulate in the water column, increasing NPP and disrupting the redox balance. The solution to this problem is to invoke a smaller supply of bioavailable phosphorus (Figure 3), such that the reduction in P burial expected in a low pO_2 environment does not result in growth of the marine P reservoir and subsequent unbalanced oxygen production.

A reduction in the Proterozoic P supply may have been mediated by increased sorptive scavenging in rivers, reducing the supply of bioavailable P to the ocean without altering the weathering rate itself (Laakso & Schrag, 2014). Inorganic scavenging from the

marine water column is not an important P sink today (e.g., Benitez-Nelson, 2000), but an increased role for such an effect would also suppress oxygen burial without violating the phosphorus budget, specifically by adding an additional sink to the P mass balance (Equation 4). Mechanisms for scavenging P from an anoxic water column include precipitation of ferruginous phosphate phases such as green rust (Halevy, Alesker, Schuster, Popovitz-Biro, & Feldman, 2017) or vivianite (Derry, 2015), and lead to stable low-oxygen conditions in global redox models (Reinhard et al., 2017). Each of these mechanisms is potentially sensitive to oxygen levels, suggesting that low-oxygen conditions sustained themselves via a positive feedback in which abundant ferrous iron suppressed the bioavailability of phosphate.

These results can be compared to simulations of Proterozoic biogeochemical cycles in a more complex biogeochemical model (Laakso & Schrag, 2017). This model is a two-box ocean with simple linear relationships between oxygen and respiration rates, but also includes remineralization processes other than oxic respiration, such as sulfate- and iron-reduction and methanogenesis, and allows for oxygen-sensitive formation of authigenic apatites. Net primary production in steady-state simulations of both eons gives primary productivity of 4 Tmol C/year, 0.1% of the simulated modern value. The supply of bioavailable P from weathering is 15% of modern, which is required to achieve stability at low pO_2 (see Section 2), so the weathering-normalized NPP is about 0.7% of the modern value, comparable to the values derived above.

Though there are no direct measurements of Proterozoic NPP with which to compare, a recent analysis of minor oxygen isotopes in sulfates suggests that the Mesoproterozoic rate of gross primary productivity (GPP) was 2–20 times slower than the modern value (Crockford et al., 2018). Though it is difficult to infer NPP from GPP in a marine ecosystem of different scale, distribution, and species composition than that of the modern ocean, a severe slow-down in GPP is consistent with a reduction in NPP, as predicted here.

4.3 | The distribution of productivity in a low-oxygen world

A tenfold to one hundredfold reduction in primary productivity implies major changes to the marine carbon cycle. The deep ocean would be starved of phosphate by the reduction in nutrient recycling: in order to decrease productivity by a factor of 100, nutrient upwelling needs to be 100 times slower than it is today, requiring deep-water phosphorus concentrations of only 20 nM (assuming identical circulation). Today, upwelling accounts for >95% of productivity, mostly into pelagic waters. Upwelling is relatively intense in coastal areas, but diffuse upwelling of deep-water phosphate still occurs widely, with 90% of productivity occurring in waters of >2,000 m depth, and 95% in waters of >200 m depth (Dunne et al., 2007). A decrease in the nutrient content of Proterozoic upwelling implies that riverine inputs of newly weathered phosphate would become a much larger fraction of total P supply to the photic zone, shifting the locus of NPP away from open waters and toward the coasts. This effect is partially offset by the reduction in weathering required to balance the P budget, described above. However, even after accounting for this effect, weathering likely drove ~30% of NPP during the Proterozoic (Figure 3), suggesting a marine biosphere more tightly distributed along coasts.

Shallow-water coastal regions are associated with more rapid sedimentation (Sadler, 1999).

The burial efficiency f_2 is less sensitive to oxygen levels in areas of high sedimentation rate (Katsev & Crowe, 2015). Furthermore, the very shallow-water column was likely weakly oxic even in the Proterozoic, when it would have been in equilibrium with an atmosphere at 1%–10% present atmospheric levels of O_2 (Lyons et al., 2014). Taking this logic to its extreme, one could argue that, if oxygen levels drop and NPP retreats toward the coasts, it becomes increasingly insensitive to the change in pO_2, acting to stabilize productivity against further changes (see related arguments made by Katsev & Crowe, 2015). The combination of these two effects does make NPP slightly less responsive to changes in the burial efficiency, as demonstrated by Figure 5. However, the net effect is to increase NPP by at most a few tens of percent over the range of burial efficiencies explored; the total drop in weathering-normalized NPP is still an order of magnitude relative to the modern day.

The low productivity biosphere described here is a steady-state solution that is consistent with low levels of pO_2 in the ocean and atmosphere. It also a stable biogeochemical cycle, as long as phosphorus inputs are held at low levels. Removing the steady-state assumption and linearizing the rates of change in the oxygen and phosphate reservoirs around the Proterozoic steady state, we find that oxygen levels are stable as long as the C_{org}:P_{Σ} ratio decreases with increasing oxygenation (see Appendix A), as is seen in modern environments (Algeo & Ingall, 2007). This negative feedback, in which rising O_2 leads to increased P retention, decreased organic carbon burial, and ultimately less oxygen production, has been invoked several times to explain the stability of Phanerozoic oxygen levels (e.g., Algeo & Ingall, 2007).

An interesting aspect of a coastally oriented biosphere is that the bulk of organic carbon cycling takes place in the oxidized surface environment, despite the continental slope and deep ocean being largely anoxic (e.g., Sperling et al., 2015). A transient increase in surface pO_2 will lead to increased nutrient regeneration and a larger marine P reservoir, which allows for more upwelling and a distribution of productivity away from the coasts and toward anoxic deep waters. This suggests that rising oxygen levels could result in organic carbon cycling shifting toward lower oxygen environments, *increasing* globally averaged P retention rates even as local shallow-water retention is depressed. Such a sequence of events is a positive feedback or at least a weakening of the negative feedback described above. Therefore, transient perturbations to pO_2 may have been only weakly suppressed, potentially allowing for large transient excursions in oxygen levels (Appendix A). Note that this behavior is a consequence of an ocean with a relatively strong depth gradient in oxidant availability, is therefore

likely to be unique to Proterozoic Eon. This may explain the observed variability of redox conditions in Neoproterozoic sections (Johnston et al., 2012). Stress resulting from variable oxygen levels has been linked to the late appearance of larger organisms relative to the Mesoproterozoic provenance of eukaryotes (Javaux, Knoll, & Malcolm, 2001), especially given the tolerance for moderate dysoxia among some modern (Sperling et al., 2013) and early (Mills et al., 2018) animals.

A retraction of nutrient supplies and net primary production toward the coasts may also help explain the decreased diversity of eukaryotes in deeper water sections of the Proterozoic (Javaux et al., 2001). Low phosphate concentrations would also have favored cyanobacteria over photosynthetic eukaryotes (Brocks et al., 2017), preventing a significant contribution to productivity from algae during the Mesoproterozoic (Knoll, Summons, Waldbauer, & Zumberge, 2007). Once oxygen levels rose, possibly following the Cryogenian glaciations as suggested by trace metal proxies (Lyons et al., 2014), and definitively by the Silurian (Sperling et al., 2015), the resulting decrease in organic carbon burial, phosphorus regeneration, and NPP, may have created more favorable conditions for the expansion of algae and other eukaryotes into a wider range of marine environments.

5 | CONCLUSIONS

Mass balance calculations presented here suggest that the global rate of net primary productivity was at least ten times smaller in the Proterozoic than today, and more likely 100 times smaller, or <50 Tmol C/year. Riverine inputs of phosphorus alone are enough to drive more than 30% of this productivity, leading to a marine biosphere that was strongly concentrated along coastal zones, and in particular near river outflows.

A predominantly coastal, shallow-water marine biosphere suggests that biogeochemical cycling may not have been exposed to the deep-water ferruginous conditions thought to have been wide-spread throughout the Proterozoic (Sperling et al., 2015). Though only the surface ocean was likely to have been oxic (Poulton et al., 2010), biogeochemical processes would have been disproportionately distributed into oxic surface waters and shallow coastal sediments. This has implications not only for carbon, phosphorus, and oxygen cycling, but for the cycles of iron and sulfate. For example, efficient burial of largely undegraded carbon in areas of rapid sedimentation should result in largely anoxic sediments with high concentrations of very labile organic carbon. This may help explain how the ocean was able to maintain sulfate reduction rates sufficient to balance sulfur inputs exclusively with pyrite burial (Fike et al., 2015), despite low concentrations of seawater sulfate.

The sedimentary record is biased toward shallow-water environments that are less likely to have been subducted on geologic timescales. The focusing of NPP toward coastal and estuarine environments means that preserved sediments are likely to record relatively high organic carbon contents or minerals and isotopic signatures associated with organic-rich sediments. Nevertheless, the Proterozoic ocean as a whole was most likely a world of limited marine life, with rates of productivity and heterotrophy at least order of magnitude smaller than today, and an open ocean that was poor in nutrients, biomass, and life.

ACKNOWLEDGMENTS

This work was supported by Henry and Wendy Breck and the Simons Foundation. Portions of this work were supported by NASA Headquarters under the NASA Earth and Space Science Fellowship Program Grant NNX11AP89H.

ORCID

Thomas A. Laakso http://orcid.org/0000-0002-2755-8050

REFERENCES

Algeo, T., & Ingall, E. (2007). Sedimentary Corg: P ratios, paleocean ventilation, and Phanerozoic atmospheric pO2. *Palaeogeography, Palaeoclimatology, Palaeoecology*, *256*, 130–155. https://doi.org/10.1016/j.palaeo.2007.02.029

Anderson, L., Delaney, M., & Faul, K. (2001). Carbon to phosphorus ratios in sediments: Implications for nutrient cycling. *Global Biogeochemical Cycles*, *15*, 65–79. https://doi.org/10.1029/2000GB001270

Benitez-Nelson, C. (2000). The biogeochemical cycling of phosphorus in marine systems. *Earth-Science Reviews*, *51*, 109–135. https://doi.org/10.1016/S0012-8252(00)00018-0

Brocks, J., Jarrett, A., Sirantoine, E., Hallmann, C., Hoshino, Y., & Liyanage, T. (2017). The rise of algae in Cryogenian oceans and the emergence of animals. *Nature*, *548*, 578–581. https://doi.org/10.1038/nature23457

Canfield, D. (1994). Factors influencing organic carbon preservation in marine sediments. *Chemical Geology*, *114*, 315–329. https://doi.org/10.1016/0009-2541(94)90061-2

Colman, A., & Holland, H. (2000). The global diagenetic flux of phosphorus from marine sediments to the oceans: Redox sensitivity and the control of atmospheric oxygen levels. In C. Glenn, L. Prévôt-Lucas, & J. Lucas (Eds.), *Marine authigenesis: From global to microbial* (pp. 53–75). Tulsa, OK: Society for Sedimentary Geology. https://doi.org/10.2110/pec.00.66

Crockford, P., Hayles, J., Bao, H., Planavsky, N., Bekker, A., Fralick, P., … Wing, B. (2018). Triple oxygen isotope evidence for limited mid-Proterozoic primary productivity. *Nature*, *559*, 613–616. https://doi.org/10.1038/s41586-018-0349-y

Derry, L. (2015). Causes and consequences of mid-Proterozoic anoxia. *Geophysical Research Letters*, *42*, 8538–8546. https://doi.org/10.1002/2015GL065333

Dunne, J., Sarmiento, J., & Gnanadesikan, A. (2007). A synthesis of global particle export from the surface ocean and cycling through the ocean interior and on the seafloor. *Global Biogeochemical Cycles*, *21*, 1–16.

Field, C., Behrenfeld, M., Randerson, J., & Falkowski, P. (1998). Primary production of the biosphere: Integrating terrestrial and oceanic components. *Science*, *281*, 237–240. https://doi.org/10.1126/science.281.5374.237

Fike, D., Bradley, A., & Rose, C. (2015). Rethinking the ancient sulfur cycle. *Annual Review of Earth and Planetary Sciences*, *43*, 593–622. https://doi.org/10.1146/annurev-earth-060313-054802

Goldblatt, C., Lenton, T., & Watson, A. (2006). Bistability of atmospheric oxygen and the Great Oxidation. *Nature*, *443*, 683–686.
Habicht, K., Gade, M., Thamdrup, B., Berg, P., & Canfield, D. (2002). Calibration of sulfate levels in the Archean Ocean. *Science*, *298*, 2372–2374.
Halevy, I., Alesker, M., Schuster, E. M., Popovitz-Biro, R., & Feldman, Y. (2017). A key role for green rust in the Precambrian oceans and the genesis of iron formations. *Nature Geoscience*, *10*, 135–139.
Hartnett, H., Keil, R., Hedges, J., & Devol, A. (1998). Influence of oxygen exposure time on organic preservation in continental margin sediments. *Nature*, *391*, 572–574. https://doi.org/10.1038/35351
Hedges, J., & Keil, R. (1995). Sedimentary organic matter preservation: An assessment and speculative synthesis. *Marine Chemistry*, *49*, 81–115. https://doi.org/10.1016/0304-4203(95)00008-F
Holland, H. (1984). *The chemical evolution of the atmosphere and oceans*. Princeton, NJ: Princeton University Press.
Javaux, E., Knoll, A., & Malcolm, W. (2001). Morphological and ecological complexity in early eukaryotic ecosystems. *Nature*, *412*, 66–69. https://doi.org/10.1038/35083562
Johnston, D., Poulton, S., Goldberg, T., Segeev, V., Podkovyrov, V., Vorob'eva, N., … Knoll, A. (2012). Late Ediacaran redox stability and metazoan evolution. *Earth and Planetary Science Letters*, *335–336*, 25–35. https://doi.org/10.1016/j.epsl.2012.05.010
Kah, L., Lyons, T., & Frank, T. (2004). Low marine sulphate and protracted oxygenation of the Proterozoic biosphere. *Nature*, *431*, 834–838.
Katsev, S., & Crowe, S. (2015). Organic carbon burial efficiencies in sediments: The power law of mineralization revisited. *Geology*, *43*, 607–610. https://doi.org/10.1130/G36626.1
Kipp, M., & Stüeken, E. (2017). Biomass recycling and Earth's early phosphorus cycle. *Science Advances*, *3*, eaao4795. https://doi.org/10.1126/sciadv.aao4795
Knoll, A., Summons, R., Waldbauer, J., & Zumberge, J. (2007). The geological succession of primary producers in the oceans. In P. Falkowski & A. Knoll (Eds.), *Evolution of primary producers in the sea* (pp. 133–163). Boston, MA: Elsevier. https://doi.org/10.1016/B978-012370518-1/50009-6
Kuntz, L., Laakso, T., Schrag, D., & Crowe, S. (2015). *Geobiology*, *13*, 454–461. https://doi.org/10.1111/gbi.12141
Laakso, T., & Schrag, D. (2014). Regulation of atmospheric oxygen during the Proterozoic. *Earth and Planetary Science Letters*, *388*, 81–91. https://doi.org/10.1016/j.epsl.2013.11.049
Laakso, T., & Schrag, D. (2017). A theory of atmospheric oxygen. *Geobiology*, *15*, 366–384. https://doi.org/10.1111/gbi.12230
Laakso, T., & Schrag, D. (2018). Limitations on limitation. *Global Biogeochemical Cycles*, *32*, 486–496.
Lyons, T., Reinhard, C., & Planavsky, N. (2014). The rise of oxygen in Earth's early ocean and atmosphere. *Nature*, *506*, 307–315. https://doi.org/10.1038/nature13068
Martin, J., Knauer, G., Karl, D., & Broenkow, W. (1987). VERTEX: Carbon cycling in the northeast Pacific. *Deep-Sea Research*, *34*, 267–285. https://doi.org/10.1016/0198-0149(87)90086-0
Mills, D., Francis, W., Vargas, S., Larsen, M., Elemans, C., Canfield, D., & Worheide, G. (2018). The last common ancestor of animals lacks the HIF pathway and respired in low-oxygen environments. *eLife*, *7*, e31176. https://doi.org/10.7554/eLife.31176
Pavlov, A., & Kasting, J. (2002). Mass-independent fractionation of sulfur isotopes in Archean sediments: strong evidence for an anoxic Archean atmosphere. *Astrobiology*, *2*, 27–41.
Pavlov, A., Hurtgen, M., Kasting, J., & Arthur, M. (2003). A Methane-rich Proterozoic atmosphere? *Geology*, *31*, 87–90.
Planavsky, N., Reinhard, C., Wang, X., Thomson, D., McGoldrick, P., Rainbird, R., … Lyons, T. (2014). Low Mid-Proterozoic atmospheric oxygen levels and the delayed rise of animals. *Science*, *346*, 635–638. https://doi.org/10.1126/science.1258410
Poulton, S., & Canfield, D. (2011). Ferruginous conditions: A dominant feature of the ocean through earth's history. *Elements*, *7*, 107–112. https://doi.org/10.2113/gselements.7.2.107
Poulton, S., Fralick, P., & Canfield, D. (2010). Spatial variability in oceanic redox structure 1.8 billion years ago. *Nature Geoscience*, *3*, 486–490. https://doi.org/10.1038/ngeo889
Reinhard, C., Planavsky, N., Gill, B., Ozaki, K., Robbins, L., Lyons, T., … Konhauser, K. (2017). Evolution of the global phosphorus cycle. *Nature*, *541*, 386–389. https://doi.org/10.1038/nature20772
Ruttenberg, K., & Berner, R. (1993). Authigenic apatite formation and burial in sediments from non-upwelling, continental margin environments. *Geochimica et Cosmochimica Acta*, *57*, 991–1007. https://doi.org/10.1016/0016-7037(93)90035-U
Sadler, P. (1999). The influence of hiatuses on sediment accumulation rates. *Georesearch Forum*, *5*, 15–40.
Sperling, E., Frieder, C., Raman, A., Girguis, P., Levin, L., & Knoll, A. (2013). Oxygen, ecology, and the Cambrian radiation of animals. *Proceedings of the National Academy of Sciences of the United States of America*, *110*, 13446–13451. https://doi.org/10.1073/pnas.1312778110
Sperling, E., Wolock, C., Morgan, A., Gill, B., Kunzmann, M., Halverson, G., … Johnston, D. (2015). Statistical analysis of iron geochemical data suggests limited late Proterozoic oxygenation. *Nature*, *523*, 451–454. https://doi.org/10.1038/nature14589
Stolper, D. A., & Keller, C. B. (2018). A record of deep-ocean dissolved O_2 from the oxidation state of iron in submarine basalts. *Nature*, *553*, 323–327. https://doi.org/10.1038/nature25009
Tyrrell, T. (1999). The relative influences of nitrogen and phosphorus on oceanic primary production. *Nature*, *400*, 525–531. https://doi.org/10.1038/22941
Van Cappellen, P., & Ingall, E. (1996). Redox stabilization of the atmosphere and oceans by phosphorus-limited marine productivity. *Science*, *271*, 493–496. https://doi.org/10.1126/science.271.5248.493
Van Mooy, B., Keil, R., & Devol, A. (2002). Impact of suboxia on sinking particulate organic carbon: Enhanced carbon flux and preferential degradation of amino acids via denitrification. *Geochimica et Cosmochimica Acta*, *66*, 457–465. https://doi.org/10.1016/S0016-7037(01)00787-6

How to cite this article: Laakso TA, Schrag DP. A small marine biosphere in the Proterozoic. *Geobiology*. 2019;17:161–171. https://doi.org/10.1111/gbi.12323

APPENDIX A

Methods Appendix

A.1 | NPP/W_p IN THE TWO-COLUMN MODEL

We first calculate effective global values of the burial efficiency terms by taking a production-weighted average of the two columns:

$$f_1 = \frac{\text{C deposition on sediments}}{\text{NPP}} = \frac{f_1^A N^A + f_1^B N^B}{N^A + N^B}$$

$$f_2 = \frac{\text{organic C burial}}{\text{C deposition on sediments}} = \frac{(f_1 f_2)^A N^A + (f_1 f_2)^B N^B}{f_1^A N^A + f_1^B N^B}$$

$$\rho = \frac{\text{organic C burial}}{\text{total P burial}} = \frac{(f_1 f_2)^A N^A + (f_1 f_2)^B N^B}{\frac{(f_1 f_2)^A}{\rho^A} N^A + \frac{(f_1 f_2)^B}{\rho^B} N^B}$$

where superscripts denote the two different columns, and N is shorthand for NPP. We can define the fraction of total net primary production that takes place in coastal waters as $\sigma = N^A/N$, giving:

$$f_1 = \sigma f_1^A + (1-\sigma) f_1^B$$

$$f_2 = \frac{\sigma (f_1 f_2)^A + (1-\sigma)(f_1 f_2)^B}{f_1}$$

$$\rho = \frac{\rho^A \rho^B}{\sigma (f_1 f_2)^A \rho^B + (1-\sigma)(f_1 f_2)^B \rho^A} f_1 f_2$$

Assuming steady-state P cycling in the photic zone:

$$N = rW_P + rU$$

$$\Rightarrow U = \frac{\left(\frac{\rho}{r} - \varepsilon_{org}\right)}{\varepsilon_{org}} W_P$$

where U is the rate of P upwelling, and we have applied results from the Section 2.

Defining μ as the fraction of total upwelling that takes place in column A, $\mu = U^A/U$:

$$\sigma \equiv \frac{N^A}{N} = \frac{W_P + U^A}{W_P + U} = \left(\mu + r\frac{\varepsilon_{org}}{\rho}(1-\mu)\right)$$

Substituting the definition of ε and solving for σ yields:

$$\sigma = \frac{\mu + r(1-\mu)\left(\frac{f_1 f_2}{\rho}\right)^B}{1 - r(1-\mu)\left(\left(\frac{f_1 f_2}{\rho}\right)^A - \left(\frac{f_1 f_2}{\rho}\right)^B\right)}$$

This can be substituted into the equations for the effective global f_1, f_2, and ρ, giving a closed form for the weathering-normalized NPP via the results derived in the Section 2:

$$\frac{\text{NPP}}{W_P} = \frac{f_1 f_2}{\rho}$$

A.2 | STABILITY ANALYSIS

Letting p represent the dissolved phosphate reservoir and x the total oceanic and atmospheric O_2 inventory:

$$\dot{x} = \varepsilon_{org}\text{NPP} - g$$

$$\dot{p} = W_P - \frac{1}{\rho}\varepsilon_{org}\text{NPP}$$

Assuming that net primary production is phosphorus limited and that nutrient uptake is sufficiently rapid to maintain photic zone P concentrations near zero:

$$\text{NPP} = r\varepsilon_{org}(W_P + u \cdot p)$$

where u is the upwelling rate.

$$\dot{x} = r\varepsilon_{org}(W_P + u \cdot p) - g$$

$$\dot{p} = W_P(1-\varepsilon_P) - \varepsilon_P u \cdot p)$$

with $\varepsilon_P = (r/\rho)\varepsilon_{org}$. Taylor expanding with respect to both variables around the steady-state solution $x = x_0$, $p = p_0$:

$$\dot{x} \approx \frac{d}{dx}\dot{x}\Big|_0 (x - x_0) + \frac{d}{dp}\dot{x}\Big|_0 (p - p_0)$$

$$= (x - x_0)\left(-\frac{d}{dx}g\Big|_0 + \frac{rW_P d}{\varepsilon_P|_0 dx}\varepsilon_{org}\Big|_0\right) + (p - p_0)(ru\varepsilon_{org}|_0)$$

$$\dot{p} \approx \frac{d}{dx}\dot{p}\Big|_0 (x - x_0) + \frac{d}{dp}\dot{p}\Big|_0 (p - p_0)$$

$$= (x - x_0)\left(-W_P \frac{d}{dx}\ln\varepsilon_P\Big|_0\right) + (p - p_0)(-u\varepsilon_P|_0)$$

where $z|_0$ indicates z evaluated at $x = x_0$, $p = p_0$. Letting $y = x - x_0$ and $q = p - p_0$:

$$\begin{pmatrix}\dot{y}\\ \dot{q}\end{pmatrix} = \begin{pmatrix}-\alpha & \beta\\ \gamma & -\delta\end{pmatrix}\begin{pmatrix}y\\ q\end{pmatrix}$$

where

$$\alpha = \frac{d}{dx}g\Big|_0 - rW_P\frac{\varepsilon_{org}}{\varepsilon_P}\Big|_0 \frac{d}{dx}\ln\varepsilon_{org}\Big|_0$$

$$\beta = ru\varepsilon_{org}|_0$$

$$\gamma = -W_P\frac{d}{dx}\ln\varepsilon_P\Big|_0$$

$$\delta = u\varepsilon_P|_0$$

Note that α, β, and δ are always positive; the sign of γ is addressed below. The solutions to such a system have terms that scale as $e^{\lambda t}$, where λ are the eigenvalues of matrix above. Therefore, the steady state $x = x_0$, $p = p_0$ is stable as long as the real parts of the eigenvalues are positive.

$$2\lambda = -(\alpha + \delta) \pm ((\alpha + \delta)^2 - 4(\alpha\delta - \beta\gamma))^{1/2}$$

Negative eigenvalues can occur when $\alpha\delta < \beta\gamma$, or:

$$\frac{d}{dx}g\Big|_0 < rW_P\left(\frac{\varepsilon_{org}}{\varepsilon_P}\frac{d}{dx}\left(\ln\varepsilon_{org} - \ln\varepsilon_P\right)\right)\Big|_0$$

Noting that steady state for the entire system requires:

$$g|_0 = rW_P \frac{\epsilon_{org}}{\epsilon_P}\Big|_0$$

the condition for unstable solutions becomes

$$\frac{d}{dx} \ln g\Big|_0 < \frac{r\epsilon_{org}}{\rho^2} \frac{d}{dx}\rho\Big|_0$$

The left-hand side is always positive, which implies the system can only be unstable if:

$$\frac{d}{dx}\rho\Big|_0 > 0$$

At individual sites, ρ decreases with the oxygen concentration of the overlying water column (Algeo & Ingall, 2007), suggesting that oxygen levels are generally stable. However, a change in the distribution of organic carbon deposition may have more complex effects on the globally averaged value of ρ (see main text). Note that if the fixed point is unstable, this does not necessarily imply unbounded growth of a perturbation, as sufficiently large excursions will move the system outside of the domain in which the linearized dynamics are an accurate description of the system. Identifying this domain and the behavior outside of it will require a more detailed understanding of how the globally averaged value of ρ varies with oxygen levels.